Enantioselective Noncovalent Synthesis of Hydrogen-Bonded Double-Rosette Assemblies

Leonard J. Prins, Jeroen J. Verhage, Feike de Jong, Peter Timmerman,* and David N. Reinhoudt*[a]

Abstract: The noncovalent synthesis of enantiomerically pure hydrogen-bonded assemblies (*M*)- and (*P*)-$\mathbf{1}_3\cdot(CA)_6$ is described. These dynamic assemblies are of one single handedness (*M* or *P*), but do not contain any chiral components. They are prepared by using the "chiral memory" concept: the induction of supramolecular chirality is achieved through initial assembly with chiral barbiturates, which are subsequently replaced by achiral cyanurates. This exchange process occurs quantitatively and without loss of the *M* or *P* handedness of the assemblies. Racemization studies have been used to determine an activation energy for racemization of 105.9 ± 6.4 kJ mol^{-1} and a half-life time to racemization of 4.5 days in benzene at 18 °C. Kinetic studies have provided strong evidence that the rate-determining step in the racemization process is the dissociation of the first dimelamine component **1** from the assembly $\mathbf{1}_3\cdot(CA)_6$. In addition to this, it was found that the expelled chiral barbiturate (*R*BAR or *S*BAR) acts as a catalyst in the racemization process. Blocking the dissociation process of dimelamines **1** from assembly $\mathbf{1}_3\cdot(CA)_6$ by covalent capture through a ring-closing metathesis (RCM) reaction produces an increase of more than two orders of magnitude in the half-life time to racemization.

Keywords: enantioselectivity · hydrogen bonds · noncovalent interactions · self-assembly · supramolecular chirality

Introduction

Chiral molecules have asymmetric arrangements of atoms and form structures that are nonsuperimposable mirror images of each other. Specific mirror images (enantiomers) may be obtained from enantiomerically pure precursor compounds either through enantioselective synthesis with a chiral catalyst or by resolution of racemic mixtures of opposite enantiomers by means of crystallization or chiral chromatography. Regardless of the methods used, it is crucial that racemization is sufficiently slow to permit isolation of the enantiomerically pure compound.

Noncovalent assemblies can similarly adopt chiral supramolecular structures when the individual components arrange themselves in a dissymmetrical fashion.[1–4] Several studies have shown that supramolecular chirality (*M* or *P*) in metal-coordinated[5, 6] and hydrogen-bonded assemblies,[7, 8] or combinations of both,[9, 10] can be induced by means of chiral centers present at the periphery of the assemblies. In cases in which the assemblies are held together by relatively strong interactions, such as metal coordination, methods analogous to those used to obtain chiral molecules yield enantiomerically pure noncovalent products.[11–17] However, the resolution of assemblies formed through weak interactions, such as hydrogen-bonding, remains challenging, reflecting their lower stability and significantly higher susceptibility to racemization.

In a previous communication we described the designing of supramolecular structures $\mathbf{1}_3\cdot(CA)_6$, held together by the cooperative action of multiple H-bonds, which provide sufficient kinetic stability to allow the isolation of the pure enantiomers (Scheme 1).[18] The assemblies were synthesized enantioselectively by using the "chiral memory" concept previously employed for the enantioselective syntheses, both based on strong ionic interactions, of a porphyrin complex (Aida et al.[19]) and of a polymeric system (Yashima et al.,[20]). Very recently, a similar approach was employed by Rebek et al. for the resolution of H-bonded capsules.[21] In this paper we give a full experimental account of the enantioselective synthesis of assemblies (*M*)- and (*P*)-$\mathbf{1}_3\cdot(CA)_6$, including studies of the different thermodynamic and kinetic characteristics of barbiturate and cyanurate assemblies. In addition, we provide a detailed description of the kinetic studies that we performed to unravel the racemization mechanism. Furthermore, we show that the half-lives of these H-bonded

[a] Dr. P. Timmerman, Prof. Dr. Ir. D. N. Reinhoudt, Dr. L. J. Prins, Ir. J. J. Verhage, Dr. F. de Jong
Laboratory of Supramolecular Chemistry and Technology
MESA$^+$ Research Institute, University of Twente
P.O. Box 217, 7500 AE Enschede (The Netherlands)
Fax: (+31) 53-4894645
E-mail: smct@ct.utwente.nl

  0947-6539/02/0810-2302 $ 20.00+.50/0

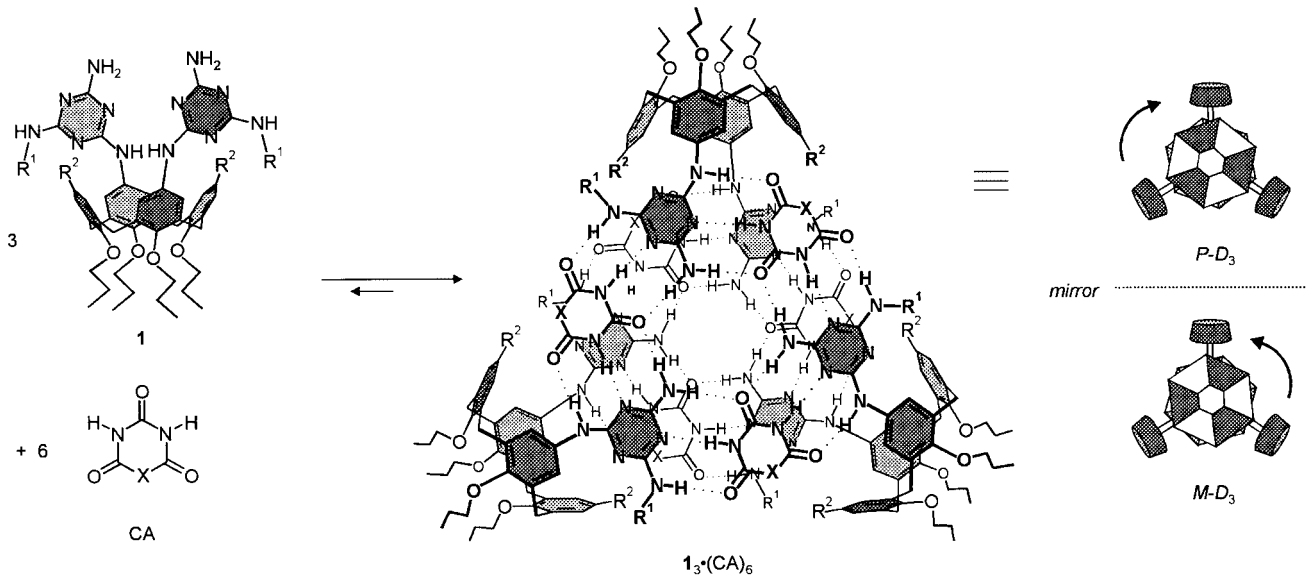

Scheme 1. Left: assembly $\mathbf{1}_3\cdot(CA)_6$ forms quantitatively upon mixing dimelamines **1** and barbiturates/cyanurates CA in a 1:2 ratio in apolar solvents such as chloroform and toluene. Right: schematic representations of the *M*-D_3 and *P*-D_3 isomers of assembly $\mathbf{1}_3\cdot(CA)_6$.

assemblies (4.5 days at 20 °C in benzene) can be increased by two orders of magnitude by covalent capture of the structure through a ring-closing metathesis (RCM) reaction.

Results and Discussion

Thermodynamic stabilities of double-rosette assemblies comprising barbiturates and cyanurates: This paper starts with a study of the thermodynamic and kinetic stabilities of assemblies $\mathbf{1}_3\cdot(CA)_6$. These studies provide important information regarding the isolation of the enantiomerically pure assemblies (*M*)-$\mathbf{1}_3\cdot(CA)_6$ and (*P*)-$\mathbf{1}_3\cdot(CA)_6$.

Previously, we described the formation of a wide variety of assemblies $\mathbf{1}_3\cdot(CA)_6$ upon mixing of dimelamines **1** with either barbiturates or cyanurates.[22–25] A crucial difference between assemblies incorporating barbiturates and those incorporating cyanurates is that cyanurates form much stronger complexes with melamines than barbiturates do. This difference in stability is clearly illustrated by comparison of the association constants for the 1:1 model complexes **2·3** and **2·4**, which (in chloroform) are $(1.0\pm0.1)\times10^2\,M^{-1}$ and $(1.5\pm0.1)\times10^4\,M^{-1}$, respectively.[26] The increased binding strength of cyanurates relative to barbiturates presumably results from the presence of the nitrogen atom, which produces a higher electron density on the carbonyl moieties and increases the acidity of the NH protons.[27–29] For that reason, the NH protons of cyanurates in assemblies $\mathbf{1}_3\cdot(CA)_6$ resonate at a much lower field ($\delta=14-16$) than barbiturates do ($\delta=13-15$).

To study the effect of the presence of barbiturates and cyanurates on the thermodynamic stability of assemblies $\mathbf{1}_3\cdot(CA)_6$, THF titration experiments were performed with assemblies $\mathbf{1a}_3\cdot(DEB)_6$ and $\mathbf{1a}_3\cdot(BuCYA)_6$ in chloroform. The polar solvent THF competes favorably with H-bond formation within the assemblies and, consequently, reduces

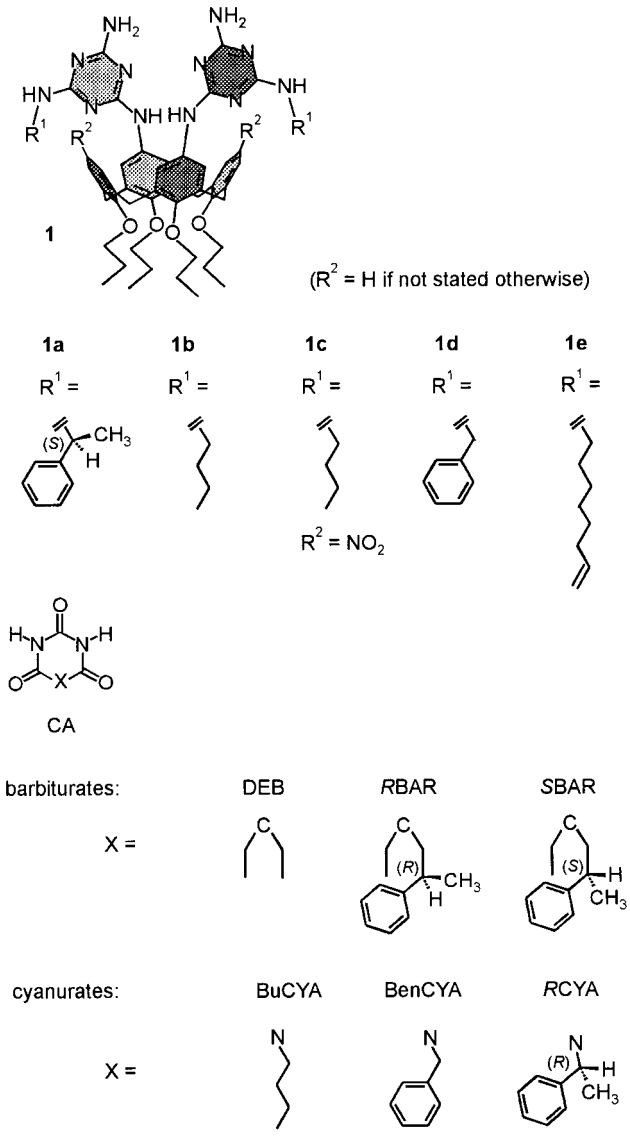

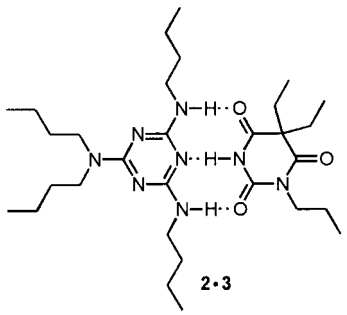

2·3

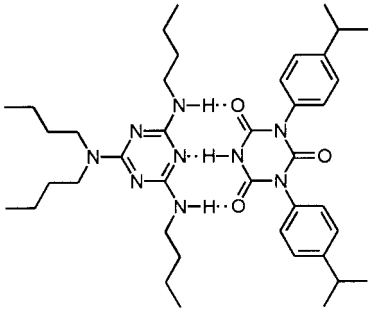

2·4

their thermodynamic stability.[30] The thermodynamic stability was evaluated in terms of the $\chi_{50\%}$ value, which represents the percentage of THF at which 50% of the assemblies are dissociated.[31, 32] The CD intensities of assemblies $\mathbf{1a}_3\cdot(\mathrm{DEB})_6$ and $\mathbf{1a}_3\cdot(\mathrm{BuCYA})_6$ were measured in $CHCl_3$/THF mixtures varying between 100:0 and 0:100. As reported previously, CD spectroscopy is a very useful tool for assessing the thermodynamic stability of these assemblies, since dissociation of the assemblies results in almost complete loss of the CD activity.[33]

From the resulting plots of relative CD intensity versus the percentage of THF, $\chi_{50\%}$ values of 11% and 95% were determined for assemblies $\mathbf{1a}_3\cdot(\mathrm{DEB})_6$ and $\mathbf{1a}_3\cdot(\mathrm{BuCYA})_6$, respectively (Figure 1). This large difference shows the enormously increased thermodynamic stability of cyanurate-based assemblies relative to assemblies that incorporate barbiturates. Even in pure THF, the CD measurements show the presence of a significant amount of $\mathbf{1a}_3\cdot(\mathrm{BuCYA})_6$ (40%). This was confirmed by ^{1}H NMR spectroscopic measurements on the assembly $\mathbf{1a}_3\cdot(\mathrm{BuCYA})_6$ in [D_8]THF, which show the characteristic H-bonded NH_{BuCYA} signals at $\delta = 14.60$ and 14.15 (Figure 2). Comparison of the integrals of these signals with those of the calix[4]arene CH_2-bridge signals of **1a** shows that 30% of $\mathbf{1a}_3\cdot(\mathrm{BuCYA})_6$ is associated, in good agreement with the CD data.

Kinetic stabilities of barbiturate and cyanurate assemblies: Despite the fact that double-rosette assemblies $\mathbf{1}_3\cdot(\mathrm{CA})_6$ are thermodynamically stable, the individual components **1** and CA are continuously in exchange. As will be shown, the higher binding affinity of cyanurates (in comparison with barbiturates) to melamines also significantly increases the kinetic stability of the assemblies.

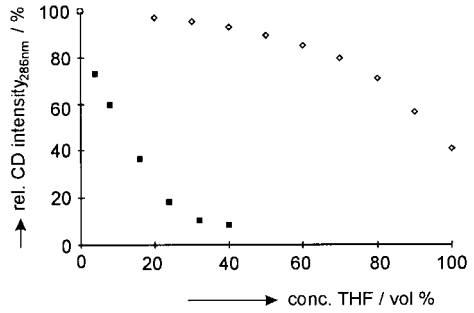

Figure 1. Relative CD intensities of solutions of assemblies $\mathbf{1a}_3\cdot(\mathrm{DEB})_6$ (■) and $\mathbf{1a}_3\cdot(\mathrm{BuCYA})_6$ (◇) in $CHCl_3$/THF plotted against the concentration of THF/vol%. Spectra were recorded at 286 nm at room temperature. The CD intensities were related to the CD intensities of assemblies $\mathbf{1a}_3\cdot(\mathrm{DEB})_6$ and $\mathbf{1a}_3\cdot(\mathrm{BuCYA})_6$ in $CHCl_3$ (1.0 mM).

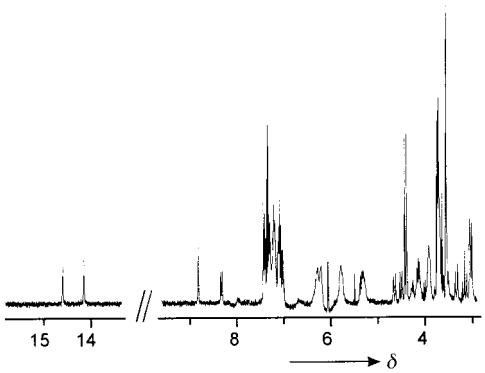

Figure 2. Part of the ^{1}H NMR spectrum of assembly $\mathbf{1a}_3\cdot(\mathrm{BuCYA})_6$ in [D_8]THF.

*Exchange rates for dimelamine components **1** from assemblies $\mathbf{1}_3\cdot(CA)_6$*: The kinetic stability of dimelamines **1** in assemblies $\mathbf{1}_3\cdot(\mathrm{DEB})_6$ can be studied by mixing solutions of homomeric assemblies $\mathbf{1b}_3\cdot(\mathrm{DEB})_6$ and $\mathbf{1c}_3\cdot(\mathrm{DEB})_6$. The heteromeric assemblies $\mathbf{1b1c}_2\cdot(\mathrm{DEB})_6$ and $\mathbf{1b}_2\mathbf{1c}\cdot(\mathrm{DEB})_6$ are formed spontaneously as a result of the interassembly exchange of dimelamines **1b** and **1c** (Scheme 2).

This process can be conveniently monitored by ^{1}H NMR spectroscopy, since the heteromeric assemblies give rise to separate signals for the NH_{DEB} protons (Figure 3).[34] The

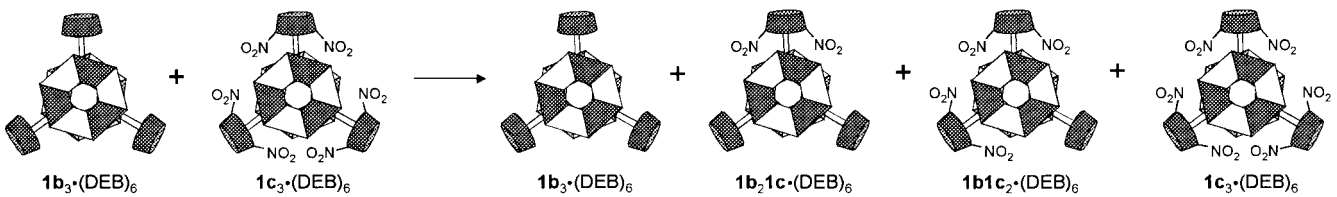

Scheme 2. Mixing of homomeric assemblies $\mathbf{1b}_3\cdot(\mathrm{DEB})_6$ and $\mathbf{1c}_3\cdot(\mathrm{DEB})_6$ results in the formation of heteromeric assemblies $\mathbf{1b1c}_2\cdot(\mathrm{DEB})_6$ and $\mathbf{1b}_2\mathbf{1c}\cdot(\mathrm{DEB})_6$ through exchange of dimelamines **1b** and **1c**.

  0947-6539/02/0810-2304 $ 20.00+.50/0 *Chem. Eur. J.* **2002**, *8*, No. 10

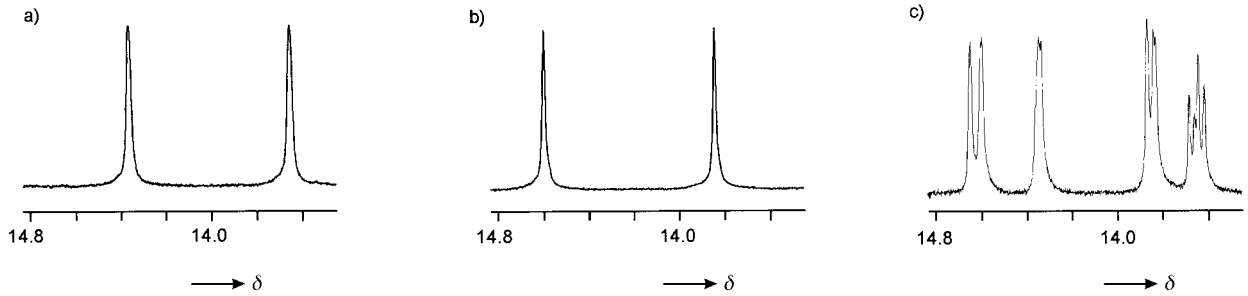

Figure 3. Sections of the ^{1}H NMR spectra of: a) $\mathbf{1b}_3\cdot(\mathrm{DEB})_6$, b) $\mathbf{1c}_3\cdot(\mathrm{DEB})_6$, and c) a mixture of $\mathbf{1b}_3\cdot(\mathrm{DEB})_6$ and $\mathbf{1c}_3\cdot(\mathrm{DEB})_6$ (1:1 ratio) recorded after 2.5 hours. All spectra were recorded in [D$_8$]toluene at room temperature. These results have been published in a preliminary communication.[35]

thermodynamic equilibrium has been reached when the ratio between the assemblies $\mathbf{1b}_n\mathbf{1c}_{3-n}\cdot(\mathrm{DEB})_6$ ($n=0-3$) does not change further. We have previously reported that, in [D$_8$]toluene, it takes 2.5 hours at room temperature before thermodynamic equilibrium is reached.[35] Two-dimensional NMR spectroscopic analyses showed that the dimelamine components **1a** and **1b** were distributed nearly statistically over the four assemblies.[36]

A much smaller exchange rate for dimelamines **1** was observed for the cyanurate-based assemblies $\mathbf{1b}_3\cdot(\mathrm{BuCYA})_6$ and $\mathbf{1c}_3\cdot(\mathrm{BuCYA})_6$. Upon mixing $\mathbf{1b}_3\cdot(\mathrm{BuCYA})_6$ and $\mathbf{1c}_3\cdot(\mathrm{BuCYA})_6$ in a 1:1 ratio in [D$_6$]benzene at 70 °C, only signals corresponding to the homomeric assemblies were observed in the ^{1}H NMR spectrum (Figure 4a–c). In time, new signals originating from the heteromeric assemblies $\mathbf{1b1c}_2\cdot(\mathrm{BuCYA})_6$ and $\mathbf{1b}_2\mathbf{1c}\cdot(\mathrm{BuCYA})_6$ slowly appeared (Figure 4d). Extrapolation with model calculations (vide infra) show that it takes 10 hours at 70 °C before thermodynamic equilibrium is reached. At room temperature, no trace of the heteromeric assemblies $\mathbf{1b}_n\mathbf{1c}_{3-n}\cdot(\mathrm{BuCYA})_6$ ($n=1-2$) was detected even after one day. This clearly illustrates the much higher kinetic stability of the cyanurate-based assemblies.

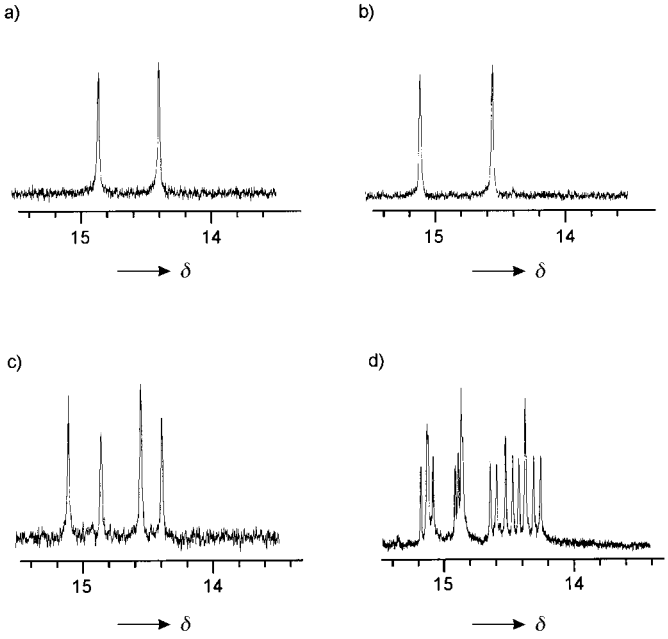

Figure 4. Sections of the ^{1}H NMR spectra of: a) assembly $\mathbf{1b}_3\cdot(\mathrm{BuCYA})_6$, b) assembly $\mathbf{1c}_3\cdot(\mathrm{BuCYA})_6$, c) a 1:1 mixture of $\mathbf{1b}_3\cdot(\mathrm{BuCYA})_6$ and $\mathbf{1c}_3\cdot(\mathrm{BuCYA})_6$ immediately after mixing, and d) the same mixture after 3 h. All spectra were recorded in [D$_6$]benzene (1.0 mM) at 70 °C.

Exchange rates for cyanurate components CA in assemblies $\mathbf{1}_3\cdot(CA)_6$: In a similar fashion, the exchange of cyanurate components was studied. Mixing of homomeric assemblies $\mathbf{1c}_3\cdot(R\mathrm{CYA})_6$ and $\mathbf{1c}_3\cdot(\mathrm{BuCYA})_6$ in a 1:1 ratio in [D$_6$]benzene at room temperature resulted in the formation of the heteromeric assemblies $\mathbf{1c}_3\cdot(R\mathrm{CYA})_n(\mathrm{BuCYA})_{6-n}$ ($n=1-5$) through exchange of the cyanurates *R*CYA and BuCYA (Scheme 3). The ^{1}H NMR spectrum recorded immediately after mixing showed the presence of numerous new signals originating from the assemblies $\mathbf{1c}_3\cdot(R\mathrm{CYA})_n(\mathrm{BuCYA})_{6-n}$ ($n=1-5$) (Figure 5c). The much faster exchange rate of cyanurates compared to dimelamines is not surprising, since only six H-bonds need to be broken in order to expel a cyanurate from the assembly. Combined with the much higher binding affinity of cyanurates—in comparison to barbitu-

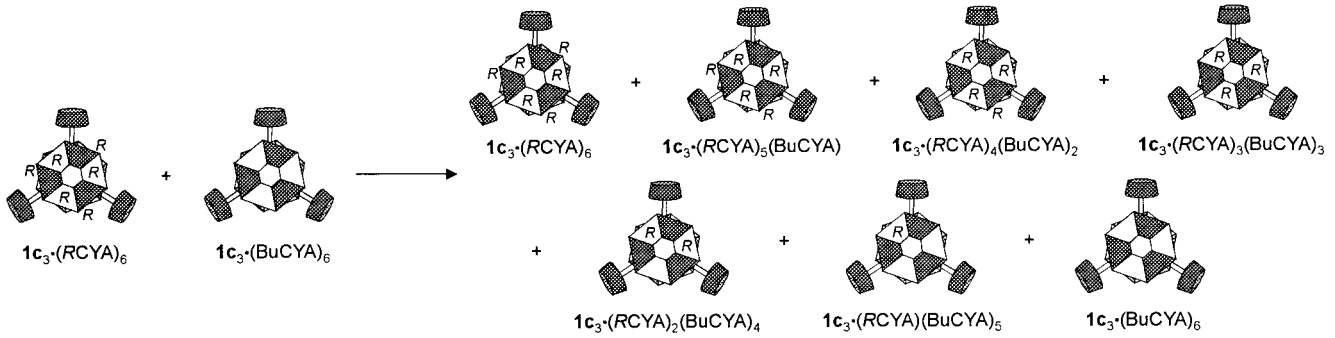

Scheme 3. Mixing of homomeric assemblies $\mathbf{1c}_3\cdot(R\mathrm{CYA})_6$ and $\mathbf{1c}_3\cdot(\mathrm{BuCYA})_6$ results in the formation of heteromeric assemblies $\mathbf{1c}_3\cdot(R\mathrm{CYA})_n(\mathrm{BuCYA})_{6-n}$ ($n=1-5$) through exchange of the cyanurate components *R*CYA and BuCYA.

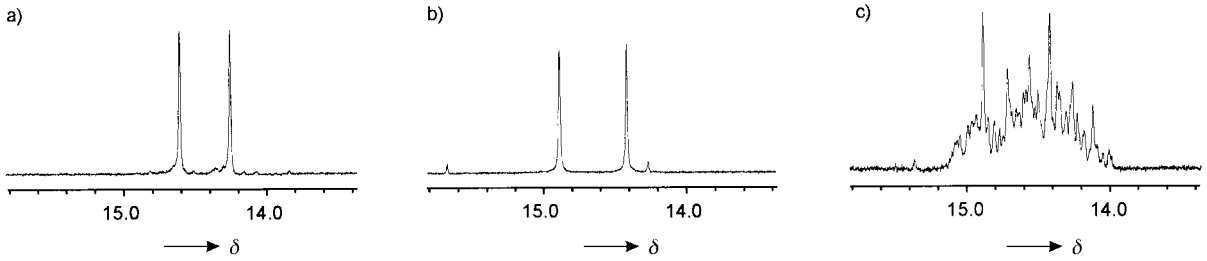

Figure 5. Sections of the ^{1}H NMR spectra of: a) $\mathbf{1c}_3\cdot(R\text{CYA})_6$, b) $\mathbf{1c}_3\cdot(\text{BuCYA})_6$, and c) a 1:1 mixture of $\mathbf{1c}_3\cdot(R\text{CYA})_6$ and $\mathbf{1c}_3\cdot(\text{BuCYA})_6$ immediately after mixing. All spectra were recorded in [D$_6$]benzene (1.0 mM) at room temperature.

rates—for melamines, this offers the possibility of applying the chiral memory concept to H-bonded assemblies $\mathbf{1}_3\cdot(\text{CA})_6$, as is shown next.

Enantioselective synthesis of hydrogen-bonded assemblies (M)-$\mathbf{1c}_3\cdot(\text{BuCYA})_6$ and (P)-$\mathbf{1c}_3\cdot(\text{BuCYA})_6$:

Exchange of a chiral barbiturate for an achiral cyanurate: Application of the chiral memory concept to assemblies $\mathbf{1}_3\cdot(\text{CA})_6$ implies the induction of supramolecular chirality through the use of chiral barbiturates, which are subsequently replaced by achiral cyanurates. We have previously reported the induction of supramolecular chirality through the use of chiral barbiturates *R*BAR and *S*BAR.[18, 37] It was found that *R*BAR nearly quantitatively induces *M* chirality in assembly $\mathbf{1c}_3\cdot(R\text{BAR})_6$ in benzene ($de = 96\,\%$). Integration of the two $\text{NH}_{R\text{BAR}}$ proton signals at $\delta = 12.69$ and 14.46 in the ^{1}H NMR spectrum revealed that these corresponded to 98% of all the signals in the $\delta = 12-15$ region. Similarly, the chiral barbiturate *S*BAR induces *P* chirality in assembly $\mathbf{1c}_3\cdot(S\text{BAR})_6$. The enantiomeric relationship between assemblies (M)-$\mathbf{1c}_3\cdot(R\text{BAR})_6$ and (P)-$\mathbf{1c}_3\cdot(S\text{BAR})_6$ is clearly reflected in their identical ^{1}H NMR spectra and mirror image CD curves (Figure 6).

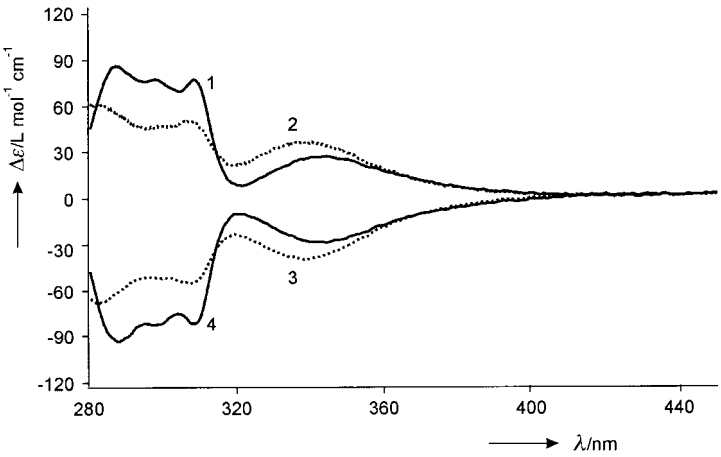

Figure 6. CD spectra of assemblies (M)-$\mathbf{1c}_3\cdot(R\text{BAR})_6$ (1), (M)-$\mathbf{1c}_3\cdot(\text{BuCYA})_6$ (2), (P)-$\mathbf{1c}_3\cdot(S\text{BAR})_6$ (3), and (P)-$\mathbf{1c}_3\cdot(\text{BuCYA})_6$ (4). All spectra were recorded in benzene (1.0 mM) at room temperature.

Subsequently, the exchange of chiral barbiturate *R*BAR for achiral cyanurate BuCYA was studied by a ^{1}H NMR titration experiment. Increasing amounts of BuCYA were added to a 1.0 mM solution of assembly (M)-$\mathbf{1c}_3\cdot(R\text{BAR})_6$ in [D$_6$]benzene. The observed changes in the $\delta = 12-15$ region of the ^{1}H NMR spectrum clearly showed that the *R*BAR units in assembly (M)-$\mathbf{1c}_3\cdot(R\text{BAR})_6$ were substituted for BuCYA units (Figure 7). The exchange was instantaneous, since the spectral changes occurred immediately after mixing. At a 1:1.3

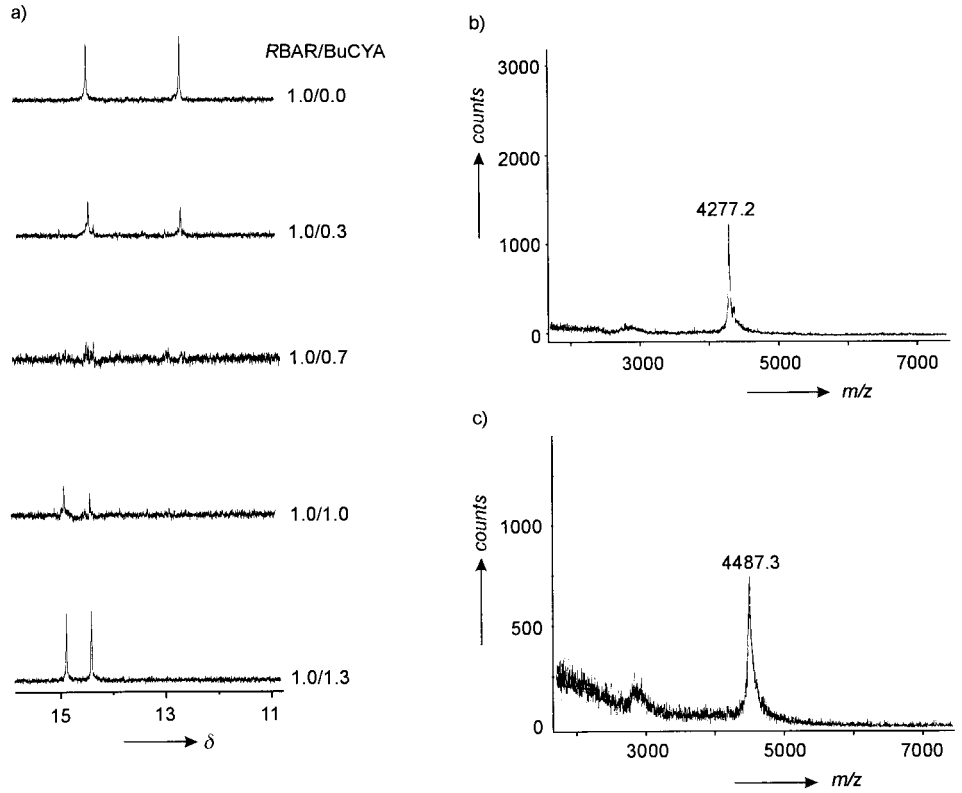

Figure 7. a) ^{1}H NMR titration of assembly (M)-$\mathbf{1c}_3\cdot(R\text{BAR})_6$ (1.0 mM) and BuCYA (amounts of BuCYA are relative to *R*BAR). All spectra were recorded at room temperature in [D$_6$]benzene. b) MALDI-TOF mass spectrum of assembly $\mathbf{1d}_3\cdot(\text{DEB})_6$ after Ag^+-labeling, and c) the same sample after the addition of 2.3 equiv. of BenCYA (relative to DEB).

  0947-6539/02/0810-2306 $ 20.00+.50/0 *Chem. Eur. J.* **2002**, *8*, No. 10

ratio of *R*BAR and BuCYA, the exchange was quantitative, as shown by the new set of signals at $\delta = 14.42$ and 14.89 for assembly $\mathbf{1c}_3\cdot(\mathrm{BuCYA})_6$ and the complete disappearance of the signals at $\delta = 12.69$ and 14.46 for assembly (*M*)-$\mathbf{1c}_3\cdot(R\mathrm{BAR})_6$.

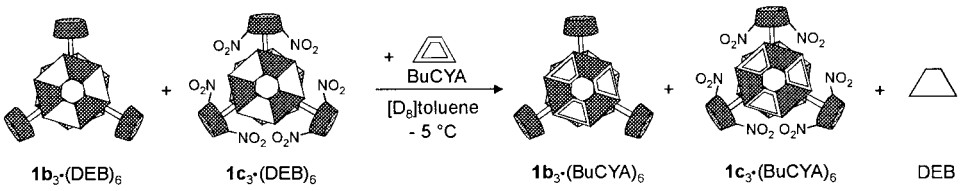

Scheme 4. Addition of 1.2 equiv. of BuCYA (relative to DEB) to a 1:1 mixture of assemblies $\mathbf{1b}_3\cdot(\mathrm{DEB})_6$ and $\mathbf{1c}_3\cdot(\mathrm{DEB})_6$ in [D_8]toluene (1.0 mM) at $-5\,^\circ$C results in the quantitative formation of assemblies $\mathbf{1b}_3\cdot(\mathrm{BuCYA})_6$ and $\mathbf{1c}_3\cdot(\mathrm{BuCYA})_6$.

Additional evidence for the fact that cyanurates quantitatively replace barbiturates was obtained from MALDI-TOF mass spectrometry measurements.[25, 38] Since assembly $\mathbf{1c}_3\cdot(\mathrm{BuCYA})_6$ lacks the essential binding site for Ag^+, an exchange experiment was performed with dimelamine **1d** and BenCYA. The MALDI-TOF mass spectrum of assembly $\mathbf{1d}_3\cdot(\mathrm{DEB})_6$ after Ag^+ labeling showed an intense signal at $m/z = 4277.2$, corresponding to the Ag^+ complex of assembly $\mathbf{1d}_3\cdot(\mathrm{DEB})_6$ (calcd for $C_{228}H_{276}O_{30}N_{48}Ag$: 4276.6; Figure 7b). After addition of 2.3 equivalents of BenCYA (relative to DEB), only a signal at $m/z = 4487.3$ was observed, corresponding to the Ag^+ complex of assembly $\mathbf{1d}_3\cdot(\mathrm{BenCYA})_6$ (calcd for $C_{240}H_{258}O_{30}N_{54}Ag$: 4486.7; Figure 7c). No signals at all were observed for assemblies $\mathbf{1d}_3\cdot(\mathrm{DEB})_n(\mathrm{BenCYA})_{6-n}$ ($n = 1-6$), in which only partial exchange of DEB for BenCYA had occurred.

Chirality memory by assembly $\mathbf{1c}_3\cdot(BuCYA)_6$: The crucial question to be answered is whether assembly $\mathbf{1c}_3\cdot(\mathrm{BuCYA})_6$, synthesized by exchange of the *R*BAR components for BuCYA in (*M*)-$\mathbf{1c}_3\cdot(R\mathrm{BAR})_6$, "memorized" the *M* chirality induced by the *R*BAR units. The CD spectrum of assembly $\mathbf{1c}_3\cdot(\mathrm{BuCYA})_6$ measured immediately after the addition of 1.2 equivalents of BuCYA (relative to *R*BAR) to assembly (*M*)-$\mathbf{1c}_3\cdot(R\mathrm{BAR})_6$ did indeed show very strong CD, despite the fact that the assembly no longer contained any chiral components (Figure 6). In a similar manner, the *P* enantiomer of assembly $\mathbf{1c}_3\cdot(\mathrm{BuCYA})_6$ was synthesized by addition of BuCYA to diastereomer (*P*)-$\mathbf{1c}_3\cdot(S\mathrm{BAR})_6$, as reflected in the opposite sign of the CD curve from that of assembly (*M*)-$\mathbf{1}_3\cdot(\mathrm{BuCYA})_6$.

Three arguments provide strong evidence that the enantiomeric excess of the assembly $\mathbf{1c}_3\cdot(\mathrm{BuCYA})_6$ must be equal to the diastereomeric excess of assembly (*M*)-$\mathbf{1c}_3\cdot(R\mathrm{BAR})_6$ (i.e., 96 %). Firstly, the observed CD intensity of the assembly (*M*)-$\mathbf{1}_3\cdot(\mathrm{BuCYA})_6$ ($\Delta\varepsilon_{max} \sim 90\ \mathrm{L\,mol^{-1}\,s^{-1}}$) is of the same magnitude as that commonly observed for similar assemblies with single handedness ($\Delta\varepsilon_{max} \sim 80-100\ \mathrm{L\,mol^{-1}\,s^{-1}}$). Secondly, at room temperature, racemization does not occur on the timescale (seconds) in which *R*BAR is exchanged for BuCYA, as shown later. Thirdly, it was shown by an additional ^{1}H NMR exchange experiment that exchange of the dimelamine components—and thus racemization (vide infra)—does not take place during barbiturate/cyanurate exchange.

Assemblies $\mathbf{1b}_3\cdot(\mathrm{DEB})_6$ and $\mathbf{1c}_3\cdot(\mathrm{DEB})_6$ were mixed in a 1:1 ratio in [D_8]toluene at $-5\,^\circ$C. Previously, it had been shown that, under these conditions, the formation of heteromeric assemblies $\mathbf{1b}_n\mathbf{1c}_{3-n}\cdot(\mathrm{DEB})_6$ ($n = 1,2$) is very slow.[35] The addition of 1.2 equivalents of BuCYA (relative to DEB) resulted in the quantitative formation of the homomeric assemblies $\mathbf{1b}_3\cdot(\mathrm{BuCYA})_6$ and $\mathbf{1c}_3\cdot(\mathrm{BuCYA})_6$ (Scheme 4), as attested to by the presence of four signals in the $\delta = 12-16$ region of the ^{1}H NMR spectrum (Figure 8). No signals were observed at all for the heteromeric assemblies $\mathbf{1b}_n\mathbf{1c}_{3-n}\cdot(\mathrm{BuCYA})_6$ ($n = 1,2$).

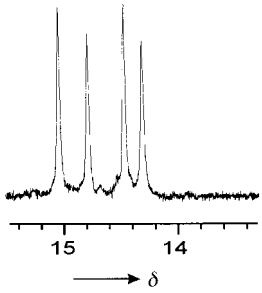

Figure 8. Section of the ^{1}H NMR spectrum after addition of BuCYA, showing that the exchange of DEB for BuCYA does not result in an exchange of dimelamines **1b** and **1c**. The spectrum was recorded at room temperature.

Several control experiments were carried out in order to exclude the possibility that the memory of chirality observed in (*M*)-$\mathbf{1c}_3\cdot(\mathrm{BuCYA})_6$ was due to the presence of free *R*BAR. First of all, it was found that the addition of free *R*BAR to the racemic assembly (*M*/*P*)-$\mathbf{1c}_3\cdot(\mathrm{BuCYA})_6$ did not give rise to CD of significant intensity ($\Delta\varepsilon_{max} < 5\ \mathrm{cm^2\,mmol^{-1}}$), even after the mixture had stood for one hour at room temperature. Moreover, the CD intensity of assembly (*M*)-$\mathbf{1c}_3\cdot(\mathrm{BuCYA})_6$ in the presence of the free *R*BAR was reduced to zero after a solution in benzene was heated at 70 °C for 45 minutes, and it was not restored after the solution had cooled to room temperature and been left to stand for an additional hour.

Activation energy for racemization: Assembly (*M*)-$\mathbf{1c}_3\cdot(\mathrm{BuCYA})_6$ is the kinetic product of the exchange reaction of *R*BAR for BuCYA in assembly (*M*)-$\mathbf{1c}_3\cdot(R\mathrm{BAR})_6$. As a result of racemization, assembly (*M*)-$\mathbf{1c}_3\cdot(\mathrm{BuCYA})_6$ will convert in time into a racemic mixture of the *M* and *P* enantiomers. In order to determine the activation energy for racemization, the racemization rate was measured by monitoring the decrease in the CD intensity over time at different temperatures (Figure 9a).

The resulting curves were fitted to the following racemization model:

$$(M)\text{-}\mathbf{1c}_3\cdot(\mathrm{BuCYA})_6 \underset{k_{rac}}{\overset{k_{rac}}{\rightleftharpoons}} (P)\text{-}\mathbf{1c}_3\cdot(\mathrm{BuCYA})_6 \qquad (1)$$

  0947-6539/02/0810-2307 $ 20.00+.50/0

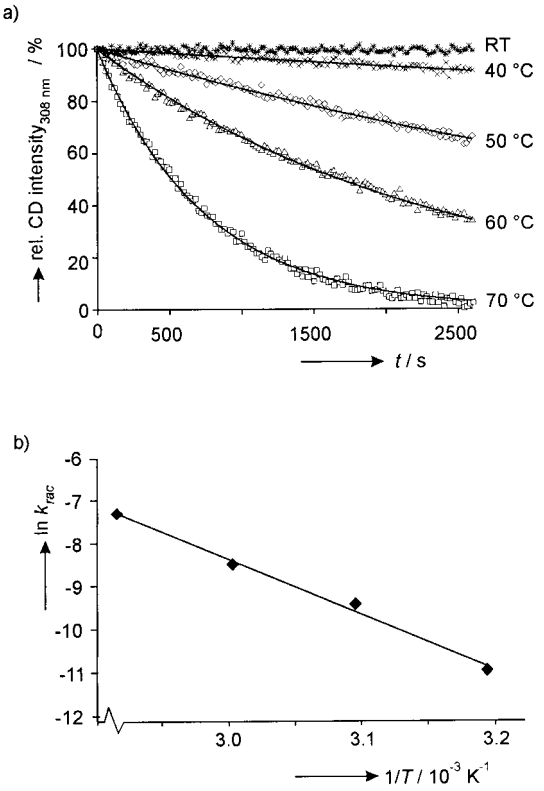

Figure 9. a) Racemization of assembly (M)-$\mathbf{1c}_3\cdot(R\text{BAR})_6$ as monitored by the decrease in CD intensity over time at various temperatures. The time-dependent measurements were started immediately after addition of 1.2 equiv. of BuCYA (relative to DEB) to a 1.0 mM solution of (M)-$\mathbf{1c}_3\cdot(R\text{BAR})_6$ in benzene at room temperature. The solid lines represent the calculated best fits of the experimental data to the racemization model described in the text. b) Arrhenius plot of $\ln k_{rac}$ versus $1/T$.

in which k_{rac} [s^{-1}] is the rate constant for racemization. Linear regression analysis gave the values for k_{rac} reported in Table 1. Subsequent analysis of these data using Arrhenius' equation (i.e., $k_{rac} = Ae^{-E_{act}/RT}$) gave an activation energy for racemization of 105.9 ± 6.4 kJ mol^{-1} (Figure 9b). The calculated half-life to racemization for assembly (M)-$\mathbf{1c}_3\cdot(\text{BuCYA})_6$ at 18 °C was found to be approximately 4.5 days. These results clearly reflect the high kinetic stability of the enantiomers of this H-bonded assembly.

Table 1. Rate constants for the racemization of the enantiomerically pure assembly (M)-$\mathbf{1c}_3\cdot(\text{BuCYA})_6$ as a function of temperature.

T [°C]	k_{rac} [10^{-5} s^{-1}]
70	67.0 ± 0.30
60	20.6 ± 0.07
50	8.2 ± 0.05
40	1.8 ± 0.03

Mechanism for the racemization of assemblies $\mathbf{1}_3\cdot(\mathbf{CA})_6$:

Kinetics of the racemization process: The enantioselective synthesis of assembly (P)-$\mathbf{1c}_3\cdot(\text{BuCYA})_6$ provides for the first time an opportunity to study the racemization mechanism of double-rosette assemblies. In principle, three species can play a role in the racemization mechanism: the assembly (P)-$\mathbf{1c}_3\cdot(\text{BuCYA})_6$ itself, the expelled *S*BAR molecules, and the BuCYA molecules present in excess. However, a possible role for free BuCYA can be ruled out because of the very low solubility of BuCYA in benzene (< 0.1 mM). Therefore, the racemization of the assembly (P)-$\mathbf{1c}_3\cdot(\text{BuCYA})_6$ was measured as a function of the initial concentrations both of assembly (P)-$\mathbf{1c}_3\cdot(\text{BuCYA})_6$ and of *S*BAR at 50 °C in benzene. The initial racemization rates, $R_{t=0}$, were determined by the racemization model described earlier:

$$R_{t=0} = -\frac{d([P - \mathbf{1c}_3\cdot(\text{BuCYA})_6])}{dt} = k_{rac}[(P)\text{-}\mathbf{1c}_3\cdot(\text{BuCYA})_6]_0 \quad (2)$$

in which k_{rac} [s^{-1}] is the overall racemization rate constant. The values of $R_{t=0}$ obtained in this way were analyzed by using:

$$R_{t=0} = k_{rac}[S\text{BAR}]_0^m[(P)\text{-}\mathbf{1c}_3\cdot(\text{BuCYA})_6]_0^n \quad (3)$$

Different initial concentrations of (P)-$\mathbf{1c}_3\cdot(\text{BuCYA})_6$ were obtained by performing the exchange of *S*BAR for BuCYA at different concentrations of (P)-$\mathbf{1c}_3\cdot(S\text{BAR})_6$. It is important to realize that in this way the concentration of expelled *S*BAR is altered as well. Therefore, the slope of 1.8 ± 0.2 found for a plot of $\ln R_{t=0}$ against $\ln[(P)\text{-}\mathbf{1c}_3\cdot(\text{BuCYA})_6]_0$ (assuming the order m in *S*BAR to be 0) cannot be directly interpreted as the order n. The influence of *S*BAR on the racemization rate (i.e., m) was studied independently by performing racemization studies at a constant initial concentration of (P)-$\mathbf{1c}_3\cdot(\text{BuCYA})_6$, in the presence of additional amounts of *S*BAR. A plot of $\ln R_{t=0}$ against $\ln[S\text{BAR}]_0$ gave a straight line with slope $m = 0.9 \pm 0.1$, this showed the active role of *S*BAR in the racemization process (Figure 10b).

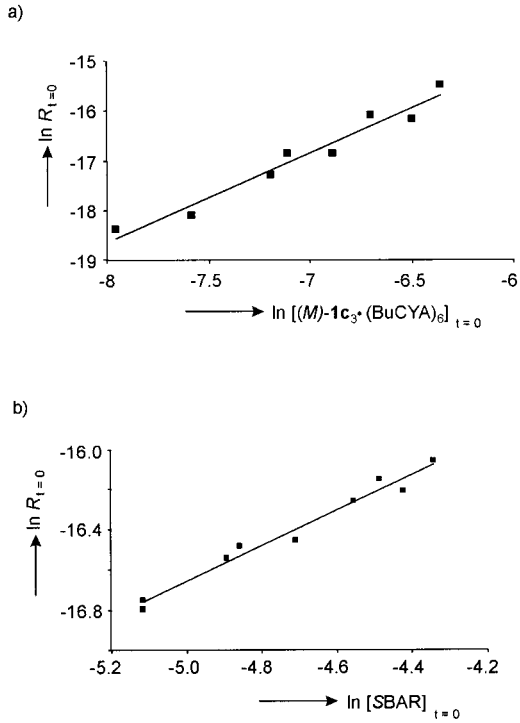

Figure 10. Dependence of the racemization rate $R_{t=0}$ on the initial concentrations of (P)-$\mathbf{1c}_3\cdot(\text{BuCYA})_6$ and *S*BAR. a) Plot of $\ln R_{t=0}$ versus $\ln[(P)\text{-}\mathbf{1c}_3\cdot(\text{BuCYA})_6]_{t=0}$, and b) plot of $\ln R_{t=0}$ versus $\ln[S\text{BAR}]_{t=0}$.

  0947-6539/02/0810-2308 $ 20.00+.50/0 *Chem. Eur. J.* **2002**, *8*, No. 10

Based on these results, the following model is proposed for the racemization of assembly $\mathbf{1c}_3\cdot(\mathrm{BuCYA})_6$:

$$(P)\text{-}\mathbf{1c}_3\cdot(\mathrm{BuCYA})_6 \underset{k_{uncat}}{\overset{k_{uncat}}{\rightleftharpoons}} (M)\text{-}\mathbf{1c}_3\cdot(\mathrm{BuCYA})_6 \quad (4)$$

$$(P)\text{-}\mathbf{1c}_3\cdot(\mathrm{BuCYA})_6 + S\mathrm{BAR} \underset{k_{cat}}{\overset{k_{cat}}{\rightleftharpoons}} (M)\text{-}\mathbf{1c}_3\cdot(\mathrm{BuCYA})_6 + S\mathrm{BAR} \quad (5)$$

this results in the following rate equation:

$$R_{t=0} = -\frac{\mathrm{d}[(P)\text{-}\mathbf{1c}_3\cdot(\mathrm{BuCYA})_6]}{\mathrm{dt}} = k_{uncat}[(P)\text{-}\mathbf{1c}_3\cdot(\mathrm{BuCYA})_6]_0 + k_{cat}[S\mathrm{BAR}][(P)\text{-}\mathbf{1c}_3\cdot(\mathrm{BuCYA})_6]_0 \quad (6)$$

Values for $k_{uncat} = (1.0 \pm 0.6) \times 10^{-5}\,\mathrm{s}^{-1}$ and $k_{cat} = (7.5 \pm 0.8) \times 10^{-3}\,\mathrm{L\,mol^{-1}\,s^{-1}}$ (at 50 °C) were determined by plotting k_{rac} versus [*S*BAR] for the concentration-dependent racemization studies discussed above (Figure 11 and Table 2). The value for k_{uncat} was determined by extrapolating k_{rac} to [*S*BAR] = 0 mM. Since only a relatively small concentration range (6–13 mM) of [*S*BAR] was studied, the k_{uncat} value has a relatively large error. Unfortunately, the nature of the exchange experiment does not allow the determination of k_{uncat} in an independent manner.

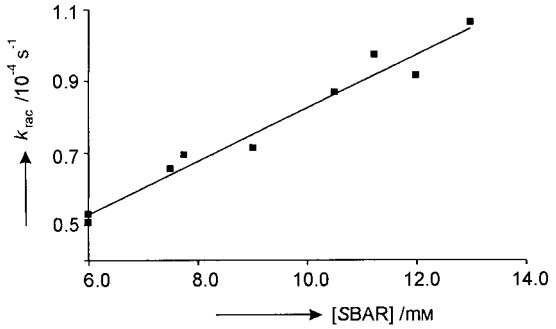

Figure 11. Determination of k_{cat} and k_{uncat} by plotting k_{obs} against [*S*BAR].

Table 2. Rate constants for the racemization of the enantiomerically pure assembly $(P)\text{-}\mathbf{1c}_3\cdot(\mathrm{BuCYA})_6$, together with exchange of dimelamine components **1c** as determined by CD and ^{1}H NMR spectroscopy, respectively.

	Method	T [°C]	k_{uncat} [10^{-5} s^{-1}]	k_{cat} [10^{-3} s^{-1}]
racemization	CD	50	1.0 ± 0.6	7.5 ± 0.8
exchange	^{1}H NMR	70	7.0 ± 0.4	16.2 ± 0.2

From the k_{cat} and k_{uncat} values it can be calculated that racemization of a 1.0 mM solution of $(P)\text{-}\mathbf{1c}_3\cdot(\mathrm{BuCYA})_6$ (and consequently 6.0 mM *S*BAR) occurs 81 % by the catalyzed pathway and only 19 % by the uncatalyzed pathway. However, this ratio is strongly concentration-dependent. For example, at 0.1 mM concentrations the uncatalyzed pathway predominates (ratio 31:69), whereas at 10 mM the uncatalyzed pathway no longer plays any significant role (ratio 98:2).

Kinetic studies on the exchange of dimelamine components ***1*** *from assemblies* $\mathbf{1}_3\cdot(BuCYA)_6$: The kinetic data obtained from the concentration-dependent CD studies do not indicate whether dissociation of the assembly is a prerequisite for racemization to occur. In order to determine whether racemization occurs intramolecularly or by a dissociative mechanism, the exchange of dimelamine components **1b** and **1c** in assemblies $\mathbf{1b}_3\cdot(\mathrm{BuCYA})_6$ and $\mathbf{1c}_3\cdot(\mathrm{BuCYA})_6$ (vide supra) was studied in more detail by ^{1}H NMR spectroscopy. Heteromeric assemblies $\mathbf{1b1c}_2\cdot(\mathrm{BuCYA})_6$ and $\mathbf{1b}_2\mathbf{1c}\cdot(\mathrm{BuCYA})_6$ can only form after dissociation of dimelamines **1b** and **1c** from the homomeric assemblies, a process that requires the disruption of twelve hydrogen bonds. Previous studies revealed that the assembly process displays strong cooperativity, and that partly-formed assemblies are completely absent.[22] Therefore, it is reasonable to assume that dissociation of the first dimelamine from the homomeric assemblies is the rate-determining step for dissociation of the assembly, and that further dissociation of the assemblies is very fast.

Assemblies $\mathbf{1b}_3\cdot(\mathrm{BuCYA})_6$ and $\mathbf{1c}_3\cdot(\mathrm{BuCYA})_6$ were mixed at different concentrations, and ^{1}H NMR spectra were recorded at regular time intervals at 70 °C in [D$_6$]benzene. The concentrations of both the homomeric and heteromeric assemblies were determined as a function of time by integration of the signals (Figure 12a). The resulting curves were fitted to a simple kinetic model in which assemblies $\mathbf{1b}_3\cdot(\mathrm{BuCYA})_6$ and $\mathbf{1c}_3\cdot(\mathrm{BuCYA})_6$ were treated as the identical species "homomer" and assemblies $\mathbf{1b1c}_2\cdot(\mathrm{BuCYA})_6$ and $\mathbf{1b}_2\mathbf{1c}\cdot(\mathrm{BuCYA})_6$ were treated as the species "heteromer". These species are in equilibrium through:

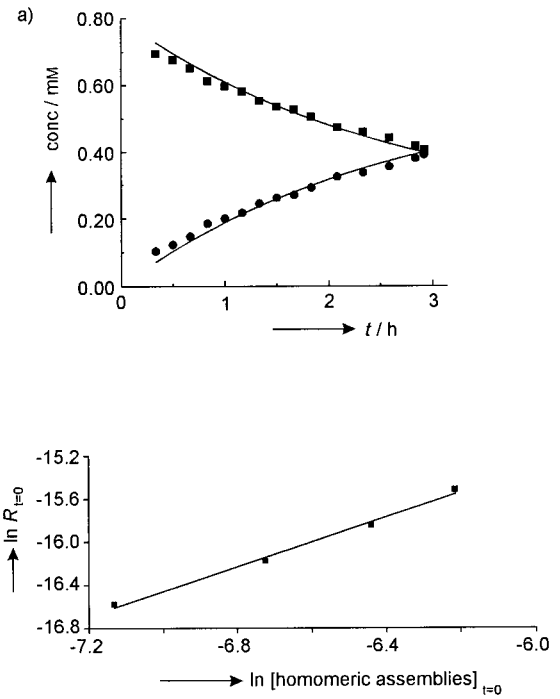

Figure 12. a) Time-dependent changes in the concentrations of homomeric assemblies $\mathbf{1b}_3\cdot(\mathrm{BuCYA})_6$ and $\mathbf{1c}_3\cdot(\mathrm{BuCYA})_6$ (■) and heteromeric assemblies $\mathbf{1b1c}_2\cdot(\mathrm{BuCYA})_6$ and $\mathbf{1b}_2\mathbf{1c}\cdot(\mathrm{BuCYA})_6$ (●) after mixing of $\mathbf{1b}_3\cdot(\mathrm{BuCYA})_6$ and $\mathbf{1c}_3\cdot(\mathrm{BuCYA})_6$ in 1:1 ratio in [D$_6$]benzene (0.8 mM) at 70 °C. The concentrations were determined by integration of the corresponding signals of the homomeric and heteromeric assemblies in the ^{1}H NMR spectrum. The lines represent the calculated best fits of the experimental data to the model described in the text. b) Plot of $\ln R_{t=0}$ versus $\ln[\mathbf{1b}_3\cdot(\mathrm{BuCYA})_6 + \mathbf{1c}_3\cdot(\mathrm{BuCYA})_6]_{t=0}$.

$$\text{homomer} \underset{k_{obs}}{\overset{3\,k_{obs}}{\rightleftharpoons}} \text{heteromer} \quad (7)$$

with k_{obs} [s^{-1}] being the rate constant. The initial rate of exchange, $R_{t=0}$, is given by:

$$R_{t=0} = -\frac{d([homomer])}{dt} = 3\,k_{obs}[homomer]^{n}_{t=0} \quad (7)$$

Linear regression analysis of the experimental data for a plot of $\ln R_{t=0}$ against $\ln$[homomer] resulted in $k_{obs} = (7.0 \pm 0.4) \times 10^{-5}\ s^{-1}$ and an order $n = 1.1 \pm 0.1$ (Figure 12b).[39]

In order to determine whether free *S*BAR accelerates the dissociation of the assemblies, additional exchange experiments were performed at constant concentrations of assemblies $\mathbf{1b}_3\cdot(BuCYA)_6$ and $\mathbf{1c}_3\cdot(BuCYA)_6$ (1.3 mM) in the presence of increasing amounts of *S*BAR (1.6–4.6 mM). Similarly to what was observed for the racemization experiments, a plot of $\ln R_{t=0}$ versus [*S*BAR] shows an increase in the dissociation rate with increasing [*S*BAR] (Figure 13a). The determined order of 0.5 ± 0.2 is on the low side, but this might be partly attributable to the fact that only three different concentrations of *S*BAR were studied. From a plot of k_{obs} versus [*S*BAR], a value for k_{cat} of $(16.2 \pm 0.2) \times 10^{-3}\ L\,mol^{-1}\,s^{-1}$ was obtained (Figure 13b).[40]

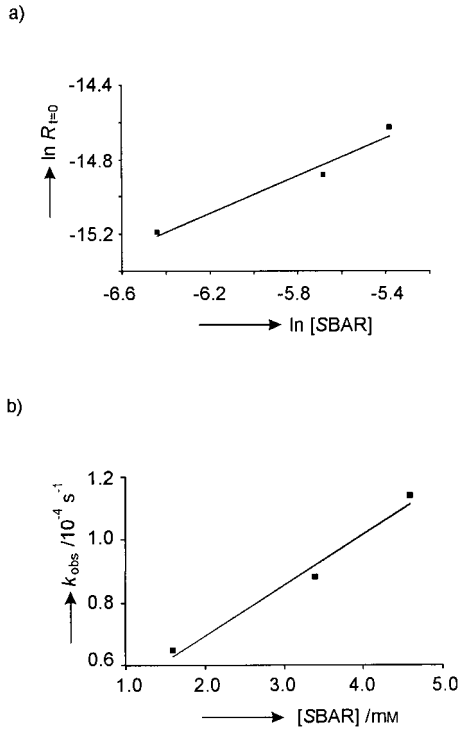

Figure 13. a) Plot of $\ln R_{t=0}$ versus $\ln$[*S*BAR], and b) determination of k_{cat} by plotting k_{obs} versus [*S*BAR].

The exchange of dimelamines **1b** and **1c** from assemblies $\mathbf{1b}_3\cdot(BuCYA)_6$ and $\mathbf{1c}_3\cdot(BuCYA)_6$ as determined from the ^{1}H NMR exchange experiments can be expressed by a rate equation similar to that used for the racemization of $\mathbf{1c}_3\cdot(BuCYA)_6$ (Table 2). The slightly higher values for dimelamine exchange are attributable to the higher temperatures at which the ^{1}H NMR experiments were conducted (70 °C) and the relatively large error in the experimentally determined order for [*S*BAR].

Proposed Mechanism of Racemization: The results of the exchange experiments strongly indicate that racemization occurs predominantly through a dissociative mechanism, both catalyzed and uncatalyzed (Scheme 5). The rate-determining step in the uncatalyzed pathway involves dissociation of the first calix[4]arene dimelamine from the intact (*P*)-$\mathbf{1c}_3\cdot(BuCYA)_6$ assembly by breaking a total of twelve hydrogen bonds. The intermediate produced (*P*)-$\mathbf{1c}_2\cdot(BuCYA)_6$ either falls apart rapidly and subsequently reassembles to give either the *M* or the *P* enantiomer, or alternatively, intermediate (*P*)-$\mathbf{1c}_2\cdot(BuCYA)_6$ racemizes quickly and immediately reforms after uptake of a dimelamine.

In the catalyzed process, formation of an activated complex (*P*)-$\mathbf{1c}_3\cdot(BuCYA)_6\cdot$(*S*BAR), resulting from (weak) association of an *S*BAR unit to assembly (*P*)-$\mathbf{1c}_3\cdot(BuCYA)_6$, precedes dissociation of the intact assembly. Binding of *S*BAR to one of the melamine DAD (donor–acceptor–donor) arrays presumably takes place. It is very unlikely that, for this interaction to occur, the melamine completely breaks all three hydrogen bonds with the BuCYA unit, because that interaction is known to be much stronger. However, interaction of the melamine with the *S*BAR could occur while the melamine–cyanurate interaction stays largely intact and is only weakened slightly. Subsequently, dissociation of the activated complex should be much faster, since breaking of the slightly weakened melamine–cyanurate H-bonds would occur more easily.

Increase of the kinetic stability through covalent capture of double rosette assemblies: We have previously shown that treatment of assembly $\mathbf{1e}_3\cdot(CA)_6$, which has six oct-1-enyl side chains, with Grubbs' catalyst in toluene results in the quantitative formation of assembly $\mathbf{5}\cdot(CA)_6$ (Scheme 6).[41, 42] A threefold RCM covalently connects the three calix[4]arene dimelamines **1e** to give macrocycle **5**. In view of the fact that dissociation of dimelamines **1** from assembly $\mathbf{1}_3\cdot(CA)_6$ is the rate-determining step in the racemization process, covalent capture of this structure would be expected to reduce the racemization rate of the H-bonded assembly significantly.

For the preparation of an enantiomerically enriched covalently captured assembly by the chiral memory concept, it is essential to induce the supramolecular chirality with a chiral barbiturate. Therefore, the assembly behavior of dimelamine **1e** with *R*BAR was studied. Comparison of the integrals of the NH_{RBAR} signals in the $\delta = 13-15$ region and the calix[4]arene CH_2 bridge protons of **1e** revealed the quantitative formation of assembly $\mathbf{1e}_3\cdot(RBAR)_6$. However, numerous signals for the NH_{RBAR} moieties were present, similarly to what had been observed for other *R*BAR-containing assemblies (Figure 14a).[37] Presumably, these signals arise from assemblies with reduced symmetry, caused by different orientations of the *R*BAR components. Although this may hardly affect the induction of supramolecular chirality by *R*BAR, this large number of signals precludes any accurate determination of the *de* of assembly $\mathbf{1e}_3\cdot(RBAR)_6$. Moreover, we cannot exactly determine the optical purity of the mixture from comparison of the CD signals with closely related assemblies, since the chromophores are in most cases not the same.[43] Therefore, a quantitative comparison is excluded. However, the maximum CD intensities of assem-

  0947-6539/02/0810-2310 $ 20.00+.50/0 *Chem. Eur. J.* **2002**, *8*, No. 10

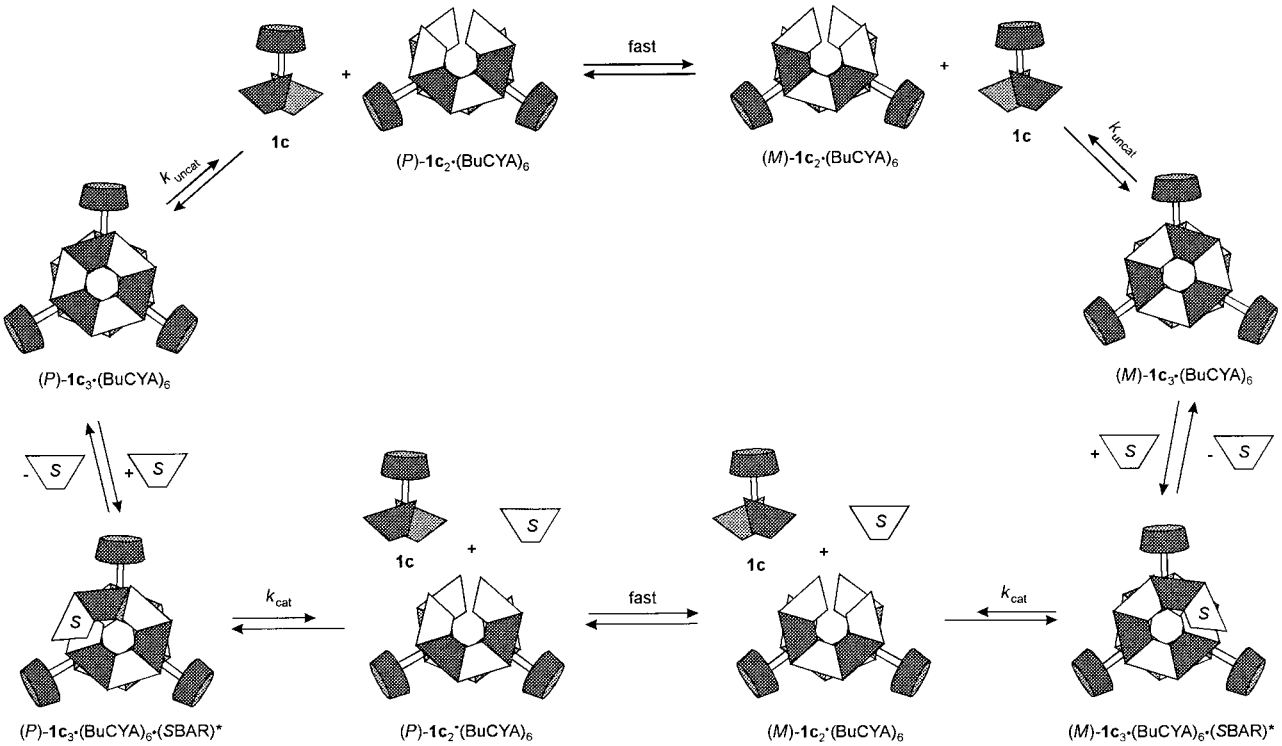

Scheme 5. Proposed mechanism for the racemization of the assembly (*P*)-**1c**$_3$·(BuCYA)$_6$. Racemization can occur both through an uncatalyzed pathway and through a catalyzed pathway in which free *S*BAR acts as a catalyst. In both pathways, the rate-determining step is dissociation of the first dimelamine **1c** from the intact assembly. This slow step is followed by rapid racemization and formation of the enantiomeric assembly (*M*)-**1c**$_3$·(BuCYA)$_6$.

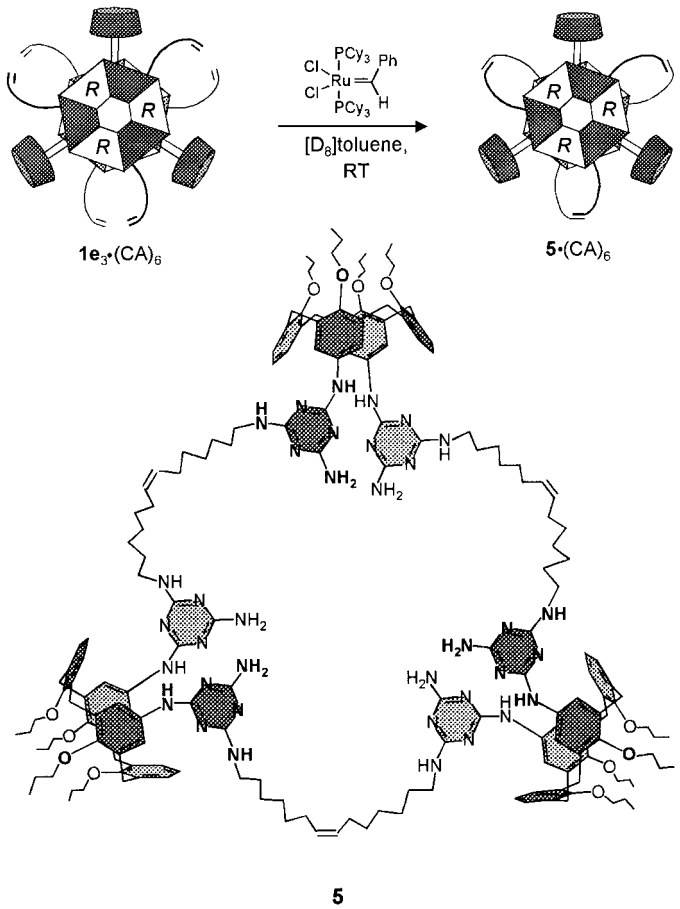

Scheme 6. Covalent capture of assemblies **1e**$_3$·(CA)$_6$ through an RCM reaction to give assembly **5**·(CA)$_6$.

blies **1e**$_3$·(*R*BAR)$_6$ ($\Delta\varepsilon_{295nm} \sim -45\,L\,mol^{-1}\,cm^{-1}$) and **5**·(BuCYA)$_6$ ($\Delta\varepsilon_{max} \sim -95\,L\,mol^{-1}\,cm^{-1}$; see Figure 14d) (vide infra) are at least comparable, in a qualitative sense, with those of the corresponding uncaptured assemblies **1c**$_3$·(*R*BAR)$_6$ and **1c**$_3$·(BuCYA)$_6$ ($\Delta\varepsilon_{max} \sim -50\,L\,mol^{-1}\,cm^{-1}$ and $\sim -90\,L\,mol^{-1}\,cm^{-1}$). Therefore, we assume that the extent of chiral induction should be more or less the same ($de \geq 80\,\%$). Actually, it is not at all important to know the exact *de* for determination of the rate constant, since the value is independent of the initial *M*/*P* ratio in the mixture.

Covalent capture of assembly **1e**$_3$·(*R*BAR)$_6$ by means of an RCM reaction was performed by addition of Grubbs' catalyst (30 mol %) to a 0.75 mM solution of **1e**$_3$·(*R*BAR)$_6$ in [D$_8$]toluene. The reaction was monitored by ^{1}H NMR spectroscopy, which showed the complete disappearance of the signals for the terminal vinylic protons of **1e** at $\delta = 5.5$ and 4.8, and the appearance of a new signal at $\delta = 5.45$, corresponding to the internal vinylic protons of assembly **5**·(*R*BAR)$_6$. Judging from the fact that the combined NH$_{RBAR}$ signals did not decrease in intensity (Figure 14b), the reaction proceeds without destruction of the assembly. After covalent capture of the H-bonded structure, the number of NH$_{RBAR}$ signals even increased, presumably due to the different steric effect imposed upon the *R*BAR units by the connected octenyl side chains. The quantitative formation of covalently captured assembly **5**·(*R*BAR)$_6$ was also evidenced by the exclusive presence of a signal at a mass-to-charge ratio of 3098 in the FAB mass spectrum, corresponding to exclusive formation of trimer **5** (calcd for $C_{180}H_{240}N_{36}O_{12} = 3098$). No signals corresponding to monomeric or dimeric structures were observed. The CD curves recorded before and after covalent capture are

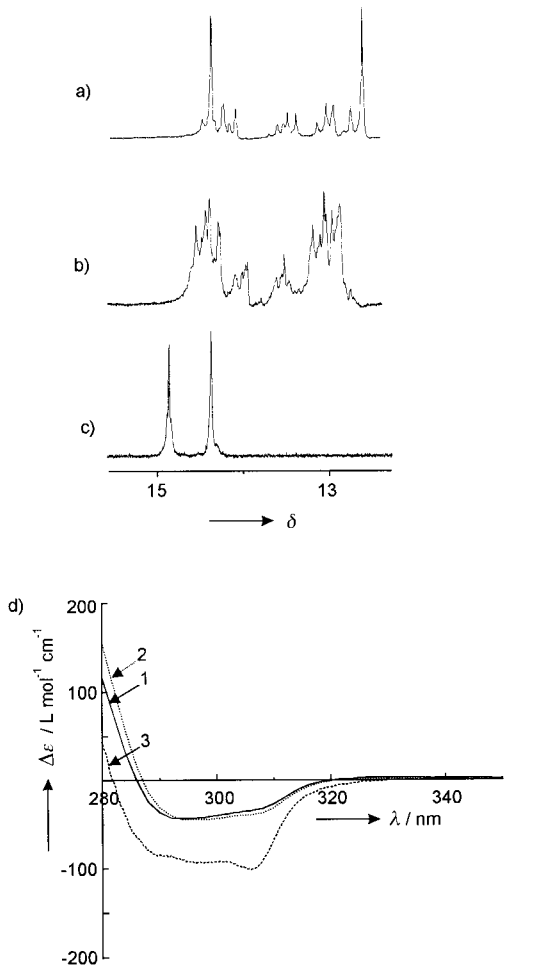

Figure 14. Sections of the ^{1}H NMR spectra of assemblies: a) $\mathbf{1e}_3\cdot(R\text{BAR})_6$, b) $\mathbf{5}\cdot(R\text{BAR})_6$, and c) $\mathbf{5}\cdot(\text{BuCYA})_6$. d) CD spectra of assemblies: $\mathbf{1e}_3\cdot(R\text{BAR})_6$ (1), $\mathbf{5}\cdot(R\text{BAR})_6$ (2), and $\mathbf{5}\cdot(\text{BuCYA})_6$ (3). All NMR and CD spectra were recorded in [D_8]toluene (0.75 mM) at room temperature.

nearly identical; this shows that assemblies $\mathbf{1e}_3\cdot(R\text{BAR})_6$ and $\mathbf{5}\cdot(R\text{BAR})_6$ have very similar *de*'s (Figure 14d).

Enantiomerically enriched assembly $\mathbf{5}\cdot(\text{BuCYA})_6$ was prepared by addition of 1.2 equiv. of BuCYA (relative to *R*BAR) to a solution of assembly $\mathbf{5}\cdot(R\text{BAR})_6$ in toluene (0.75 mM) at room temperature. The quantitative exchange of *R*BAR for BuCYA was evidenced by the exclusive presence of only two new signals at $\delta = 14.87$ and 14.38 in the $\delta = 13-15$ region of the ^{1}H NMR spectrum (Figure 14c). All signals corresponding to assembly $\mathbf{5}\cdot(R\text{BAR})_6$ had completely disappeared. Assembly $\mathbf{5}\cdot(\text{BuCYA})_6$ exhibited very strong CD activity ($\Delta\varepsilon_{300\text{nm}} = -92\ \text{L mol}^{-1}\text{cm}^{-1}$), comparable to that of the uncaptured assembly $\mathbf{1c}_3\cdot(\text{BuCYA})_6$ ($\Delta\varepsilon_{300\text{nm}} \sim -85\ \text{L mol}^{-1}\text{cm}^{-1}$); this shows that this assembly had also quantitatively "memorized" the chirality induced by the *R*BAR components.

Racemization of the enantiomerically (almost) pure assembly (*P*)-$\mathbf{5}\cdot(\text{BuCYA})_6$ was monitored by measuring the decrease in CD intensity (300 nm) as a function of time at 70 °C (Figure 15). Fitting the curve to our model for racemization (vide supra) resulted in a value of $k_{rac} = (1.0 \pm 0.1) \times 10^{-6}\ \text{s}^{-1}$ and a corresponding half-life to racemization of

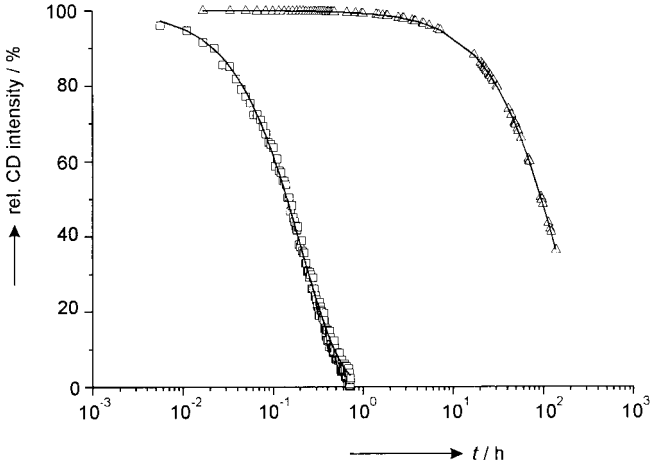

Figure 15. CD spectra showing the racemization of (*P*)-$\mathbf{5}_3\cdot(\text{BuCYA})_6$ (□) and $\mathbf{1c}_3\cdot(\text{BuCYA})_6$ (△) over time. Spectrum measured at 300 nm and 70 °C.

95 hours (~4 days). Comparison with the half-life of uncaptured assembly $\mathbf{1c}_3\cdot(\text{BuCYA})_6$—0.14 hours under similar conditions (benzene, 70 °C)—shows that covalent capture of the assembly decreases the racemization rate by a factor of 650. The high kinetic stability of assembly $\mathbf{5}\cdot(\text{BuCYA})_6$ is emphasized by the fact that the CD intensity had decreased by only 9 % after two weeks at room temperature in toluene.

These results clearly show that blocking the dissociative racemization pathway by covalent capture decreases the racemization rate by more than two orders of magnitude. The racemization mechanism of the captured assembly is unknown at present, but most likely involves an intra-assembly rearrangement in which most of the 36 hydrogen bonds have to be broken.

Conclusion

The enantiomerically pure H-bonded assembly $\mathbf{1c}_3\cdot(\text{BuCYA})_6$ has been prepared by the "chiral memory" concept: induction of supramolecular chirality is achieved with chiral barbiturates, which are subsequently replaced by achiral cyanurates in a qualitative manner. The success of this approach relies primarily on the association between cyanurates and melamines being much stronger than that between barbiturates and melamines and the very low dissociation rate of dimelamine **1c** from the double-rosette assembly $\mathbf{1c}_3\cdot(\text{BuCYA})_6$. Racemization studies revealed an activation energy for racemization of $105.9 \pm 6.4\ \text{kJ mol}^{-1}$ and a half-life of 4.5 days in benzene at 18 °C. These values clearly reflect the remarkably high stability of these H-bonded assemblies, which results from the cooperative action of multiple weak interactions. Kinetic studies have provided strong evidence that dissociation of the first dimelamine **1c** from assembly $\mathbf{1c}_3\cdot(\text{BuCYA})_6$ is the rate-determining step in the racemization process. Remarkably, a catalytic role was observed for the expelled barbiturate, which presumably enhances the dissociation of dimelamines **1c** through the formation of an "activated" complex with assembly $\mathbf{1c}_3\cdot(\text{BuCYA})_6$.

The kinetic stability of the assemblies was increased significantly by covalent capture of the H-bonded structure

  0947-6539/02/0810-2312 $ 20.00+.50/0 *Chem. Eur. J.* **2002**, *8*, No. 10

through an RCM reaction, which connects the three dimelamine components **1e** to give the assembly **5**·(BuCYA)$_6$. In this way the dissociative racemization pathway was blocked; this resulted in a half-life to racemization of ~4 days in toluene at 70 °C. Relative to assemblies **1c**$_3$·(BuCYA)$_6$, the half-life has been increased by *more than two orders of magnitude*.

Experimental Section

The syntheses of dimelamine **1a**,[24] barbiturates *R*BAR and *S*BAR,[37] and BuCYA[24] have been described elsewhere. Dimelamines **1b–e** and model compounds **2–4** were prepared according to literature procedures.[23, 26, 41] Barbiturate DEB was obtained from Fluka.

***N*-(Benzyl)imidocarbonic acid**: *N*-(Benzyl)imidocarbonic acid was prepared by following the procedure for the synthesis of *N*-[(*R*)-1-phenylethyl]imidocarbonic acid.[37]

***N*-(Benzyl)-1,3,5-triazine-2,4,6(1H,3H,5H)-trione (BenCYA)**: BenCYA was prepared by following the procedure for the synthesis of cyanurate *R*CYA, with *N*-(benzyl)imidocarbonic acid as an intermediate.[37]

Barbiturate–cyanurate exchange experiments: Typically, a solution of BuCYA (15 mM, 500 μL, obtained after sonication at elevated temperatures) in benzene was added to a solution of assembly **1**$_3$·(BAR)$_6$ in benzene (6.0 mM, 100 μL). CD and ^{1}H NMR measurements at variable temperatures were performed immediately after the components had been mixed.

Metathesis reaction: The metathesis reactions were performed by following the previously published procedure.[24, 41]

Acknowledgement

The authors would like to acknowledge R. Fokkens and Prof. N. M. M. Nibbering for the MALDI-TOF MS measurements. This research was financially supported by the Council for Chemical Sciences of the Netherlands Organization for Scientific Research (CW-NWO).

[1] *Templating, Self-Assembly, and Self-Organization, Vol. 9*, Pergamon, Oxford, UK, **1996**.
[2] G. M. Whitesides, E. E. Simanek, J. P. Mathias, C. T. Seto, D. N. Chin, M. Mammen, D. M. Gordon, *Acc. Chem. Res.* **1995**, *28*, 37–44.
[3] D. Philp, J. F. Stoddart, *Angew. Chem.* **1996**, *108*, 1242–1286; *Angew. Chem. Int. Ed. Engl.* **1996**, *35*, 1154–1194.
[4] L. J. Prins, D. N. Reinhoudt, P. Timmerman, *Angew. Chem.* **2001**, *113*, 2446–2492; *Angew. Chem. Int. Ed.* **2001**, *40*, 2383–2426.
[5] W. Zarges, J. Hall, J.-M. Lehn, A. De Cian, J. Fischer, *Helv. Chim. Acta* **1991**, *74*, 1843–1852.
[6] C. Piguet, G. Bernardinelli, G. Hopfgartner, *Chem. Rev.* **1997**, *97*, 2005–2062.
[7] a) R. K. Castellano, B. H. Kim, J. Rebek Jr., *J. Am. Chem. Soc.* **1997**, *119*, 12671–12672; b) J. Rivera, T. Martín, J. Rebek Jr., *Science* **1998**, *279*, 1021–1023.
[8] E. E. Simanek, S. Qiao, I. S. Choi, G. M. Whitesides, *J. Org. Chem.* **1997**, *62*, 2619–2621.
[9] A. L. Marlow, E. Mezzina, G. P. Spada, S. Masiero, J. T. Davis, G. Gottarelli, *J. Org. Chem.* **1999**, *64*, 5116–5123.
[10] X. D. Shi, J. C. Fettinger, J. T. Davis, *J. Am. Chem. Soc.* **2001**, *123*, 6738–6739.
[11] C. R. Woods, M. Benaglia, F. Cozzi, J. S. Siegel, *Angew. Chem.* **1996**, *108*, 1977–1980; *Angew. Chem. Int. Ed. Engl.* **1996**, *35*, 1830–1833.
[12] L. J. Charbonnière, M.-F. Gilet, K. Bernauer, A. F. Williams, *Chem. Commun.* **1996**, 39–40.
[13] L. J. Charbonnière, G. Bernardinelli, C. Piguet, A. M. Sargeson, A. F. Williams, *Chem. Commun.* **1994**, 1419–1420.
[14] B. Hasenknopf, J.-M. Lehn, *Helv. Chim. Acta* **1996**, *79*, 1643–1650.
[15] F. R. Keene, *Chem. Soc. Rev.* **1998**, *27*, 185–193.
[16] G. Rapenne, B. T. Patterson, J.-P. Sauvage, F. R. Keene, *Chem. Commun.* **1999**, 1853–1854.
[17] A. Werner, M. Michels, L. Zander, J. Lex, E. Vogel, *Angew. Chem.* **1999**, *111*, 3866–3870; *Angew. Chem. Int. Ed.* **1999**, *38*, 3650–3653.
[18] L. J. Prins, F. De Jong, P. Timmerman, D. N. Reinhoudt, *Nature* **2000**, *408*, 181–184.
[19] Y. Furusho, T. Kimura, Y. Mizuno, T. Aida, *J. Am. Chem. Soc.* **1997**, *119*, 5267–5268.
[20] E. Yashima, K. Maeda, Y. Okamoto, *Nature* **1999**, *399*, 449–451.
[21] J. M. Rivera, S. L. Craig, T. Martín, J. Rebek Jr., *Angew. Chem.* **2000**, *112*, 2214–2216; *Angew. Chem. Int. Ed.* **2000**, *39*, 2130–2132.
[22] R. H. Vreekamp, J. P. M. Van Duynhoven, M. Hubert, W. Verboom, D. N. Reinhoudt, *Angew. Chem.* **1996**, *108*, 1306–1309; *Angew. Chem. Int. Ed. Engl.* **1996**, *35*, 1215–1218.
[23] P. Timmerman, R. H. Vreekamp, R. Hulst, W. Verboom, D. N. Reinhoudt, K. Rissanen, K. A. Udachin, J. Ripmeester, *Chem. Eur. J.* **1997**, *3*, 1823–1832.
[24] L. J. Prins, K. A. Jolliffe, R. Hulst, P. Timmerman, D. N. Reinhoudt, *J. Am. Chem. Soc.* **2000**, *122*, 3617–3627.
[25] P. Timmerman, K. A. Jolliffe, M. Crego Calama, J.-L. Weidmann, L. J. Prins, F. Cardullo, B. H. M. Snellink-Ruel, R. Fokkens, N. M. M. Nibbering, S. Shinkai, D. N. Reinhoudt, *Chem. Eur. J.* **2000**, *6*, 4104–4115.
[26] A. G. Bielejewska, C. E. Marjo, L. J. Prins, P. Timmerman, F. De Jong, D. N. Reinhoudt, *J. Am. Chem. Soc.* **2001**, *123*, 7518–7533.
[27] H. S. Shieh, D. Voet, *Acta Crystallogr. Sect. B: Struct. Sci.* **1976**, *32*, 2354–2360.
[28] M. Mascal, P. S. Fallon, A. S. Batsanov, B. R. Heywood, S. Champ, M. Colclough, *J. Chem. Soc. Chem. Commun.* **1995**, 805–806.
[29] O. Félix, personal communication.
[30] In principle, the intrinsic CD intensities of assemblies **1a**$_3$·(DEB)$_6$ and **1a**$_3$·(BuCYA)$_6$ could be solvent-dependent; this would result in slightly different relative CD intensities. However, this solvent effect is assumed to be equal for both assemblies.
[31] M. Mammen, E. E. Simanek, G. M. Whitesides, *J. Am. Chem. Soc.* **1996**, *118*, 12614–12623.
[32] J. K. M. A. Kerckhoffs, M. Crego Calama, I. Luyten, P. Timmerman, D. N. Reinhoudt, *Org. Lett.* **2000**, *2*, 4121–4124.
[33] L. J. Prins, C. Thalacker, F. Würthner, P. Timmerman, D. N. Reinhoudt, *Proc. Natl. Acad. Sci. USA* **2001**, *98*, 10042–10045.
[34] The heteromeric assemblies **1b1c**$_2$·(DEB)$_6$ and **1b**$_2$**1c**·(DEB)$_6$ give rise to six signals for the NH$_{DEB}$ protons as a result of the reduced symmetry of the assembly.
[35] M. Crego Calama, R. Fokkens, N. M. M. Nibbering, P. Timmerman, D. N. Reinhoudt, *Chem. Commun.* **1998**, 1021–1022.
[36] The statistical ratio of assemblies **1b**$_3$·(DEB)$_6$, **1b1c**$_2$·(DEB)$_6$, **1b**$_2$**1c**·(DEB)$_6$, and **1c**$_3$·(DEB)$_6$ in the mixture is 1:3:3:1.
[37] L. J. Prins, R. Hulst, P. Timmerman, D. N. Reinhoudt, *Chem. Eur. J.* **2001**, *8*, 2288–2301.
[38] K. A. Jolliffe, M. Crego Calama, R. Fokkens, N. M. M. Nibbering, P. Timmerman, D. N. Reinhoudt, *Angew. Chem.* **1998**, *110*, 1294–1297; *Angew. Chem. Int. Ed.* **1998**, *37*, 1247–1251.
[39] In the model, the dissociation rates of dimelamines **1b** and **1c** are assumed to be equal. However, this might not be the case, which may possibly explain the slight mismatch between experimental and calculated data.
[40] A value for k_{uncat} of $(3.7 \pm 0.8) \times 10^{-5}$ s^{-1} was obtained from these experiments, and corresponds very well to the value of $(7.0 \pm 0.4) \times 10^{-5}$ s^{-1} that was obtained directly.
[41] F. Cardullo, M. Crego Calama, B. H. M. Snellink-Ruël, J.-L. Weidmann, A. Bielejewska, R. Fokkens, N. M. M. Nibbering, P. Timmerman, D. N. Reinhoudt, *Chem. Commun.* **2000**, 367–368.
[42] Macrocycle **5** is only formed if assembly **1**$_3$·(CA)$_6$ is present as the D_3 isomer. An RCM reaction performed on assemblies **1**$_3$·(CA)$_6$ with C_{3h} and C_s symmetry results in the exclusive formation of intramolecularly closed monomer; see also ref. [41].
[43] It is remarkable to note that *R*BAR induces *P* chirality in assembly **1e**$_3$·(*R*BAR)$_6$ and *M* chirality in assembly **1c**$_3$·(*R*BAR)$_6$ (see also ref. [37]). This difference is attributed to the NO_2 substituents present in **1c**.

Received: October 12, 2001 [F3609]